Draft version February 1, 2008
Preprint typeset using LaTeX style emulateapj v. 10/09/06

THE KINETIC SUNYAEV-ZEL'DOVICH EFFECT DUE TO THE ELECTRONS OF OUR GALAXY

Amir Hajian[1,2], Carlos Hernández-Monteagudo[3], Raul Jimenez[3], David Spergel[2], Licia Verde[3]

Draft version February 1, 2008

ABSTRACT

We compute the effect of local electrons on the CMB temperature anisotropies. The number density and distribution of free electrons in our Galaxy has been accurately measured from pulsar dispersion measurements. Because of their distribution, the dynamics of our Galaxy and the Galaxy peculiar velocity with respect to the Hubble flow, these free electrons leave a frequency-independent imprint on the cosmic microwave background (CMB). In particular, the coherent motion of the free electrons respect to us and to the CMB rest frame produce a kinetic Sunyaev-Zeldovich signal. We compute this effect and we note that the large-scale antisymmetry of the signal gives it an angular power spectrum with a sawtooth pattern where even multipoles are suppressed with respect to the odd ones. We find the signal to be small ($\sim 2\mu K$) and sub-dominant compared to the primary CMB and other foreground signals. However, since there are no free parameters in the modeling of this signal, it can be taken into account if more precise measurements of the primordial signal are required.

Subject headings: Cosmology: cosmic microwave background — Galaxy: kinematics and dynamics

1. INTRODUCTION AND BACKGROUND

The motion of the ionized gas in our Galaxy leaves its imprint on the CMB through the Kinetic Sunyaev-Zeldovich Effect (Sunyaev & Zeldovich 1980; Hogan 1992). These distortions are spectrally indistinguishable from the CMB. Thompson scattering of CMB photons from a line element ds of free electrons with optical depth $d\tau$ along the line of sight determined by the unit vector $\hat{\mathbf{n}}$, gives a correction to the CMB temperature:

$$dT(\hat{\mathbf{n}}) = -d\tau \delta T_{CMB}(\hat{\mathbf{n}}) - d\tau \frac{\mathbf{v}}{c} \cdot \hat{\mathbf{n}} T_{CMB}(\hat{\mathbf{n}}). \quad (1)$$

Thus there are two terms, the first is a blurring of the CMB anisotropies ($\delta T_{CMB}(\hat{\mathbf{n}}) = T_{CMB}(\hat{\mathbf{n}}) - T_0$ where $T_0 = \langle T_{CMB} \rangle$), while the second is a generation of new anisotropies: the kinetic SZ (kSZ) effect.

If $\delta T_{CMB} \ll T_0$ (i.e., we are in a coordinate system where the CMB has zero dipole[4]) and $v/c > 10^{-5}$, the second term dominates. Thus the integrated effect along the line of sight, for $\tau \ll 1$ is given by:

$$\frac{\delta T}{T} = -\int n_e \sigma_T \frac{v_r}{c} dl \sim \tau(\hat{\mathbf{n}}) \frac{v_r(\hat{\mathbf{n}})}{c} \quad (2)$$

where $v_r \equiv \mathbf{v} \cdot \hat{\mathbf{n}}$, n_e denotes the electron density and σ_T the Thompson cross section. Given that plausible velocities are of the orders of few $\times 100$ km/s (the largest velocity, 620 km/s, is that of the infall of the local group to the Great Attractor) only $\tau > 10^{-3}$ yields a measurable signal. Such high optical depth implies a number density of electrons and baryonic mass that is only consistent with that present in the disk of our own Galaxy.

In this case, the velocity can be written as a sum of the Sun's velocity as measured from the CMB dipole, $v_{\rm dipole}$, and the gas velocity with respect to the Sun. Note that in a coordinate system where the Sun is at rest, the contribution for $v_{\rm dipole}$ is interpreted as a blurring of anisotropies (first term in the LHS of eq 1), the anisotropies being the CMB dipole.

Here, we compute the kSZ signature of the Galaxy on the CMB sky. While this signal is sub-dominant compared to other foreground signals and small compared to the intrinsic CMB anisotropy, it is a component that must be there and that can be modeled as we illustrate below. We assume a simple model for the velocities of the free electrons in our Galaxy that includes an axisymmetric model for the rotation around the Galactic center with the same speed as the luminous matter, $\mathbf{v}_{rot}$, and a bulk motion, $\mathbf{v}_{bulk}$ of the galactic center with respect to the Hubble flow. We neglect the higher order corrections to these assumptions such as blurring of intrinsic CMB anisotropies (first term in eq. 1). The total velocity of the free electrons with respect to the CMB rest frame is the vector sum of the above velocities, $\mathbf{v} = \mathbf{v}_{rot} + \mathbf{v}_{bulk}$. The bulk velocity, $\mathbf{v}_{bulk}$, can be derived from the observed dipole of the CMB as $\mathbf{v}_{bulk} = \mathbf{v}_{dipole} - \mathbf{v}_\odot$, where $\mathbf{v}_\odot$ is the linear velocity of the rotation of the Sun around the galactic center. Therefore we have $\mathbf{v} = \mathbf{v}_{dipole} + (\mathbf{v}_{rot} - \mathbf{v}_\odot)$. The radial part of this velocity is the v_r that appears in eqn.(2) and is given by

$$v_r = v_{los} + \mathbf{v}_{dipole} \cdot \hat{\mathbf{n}}, \quad (3)$$

where $v_{los} = (\mathbf{v}_{rot} - \mathbf{v}_\odot) \cdot \hat{\mathbf{n}}$ is the line-of-sight velocity with respect to the Sun.

2. THE MODEL FOR THE GALACTIC DISTRIBUTION OF FREE ELECTRONS

We use the Cordes and Lazio (Cordes & Lazio 2002) model (hereafter NE2001) for the distribution of free electrons in our Galaxy. Cordes & Lazio (2002) combine the measurements of the dispersion measures (DM) of pulsars, temporal broadening of pulses from pulsars with large DM, scintillation bandwidth measurements of

[1] Department of Physics, Jadwin Hall, Princeton University, Princeton, NJ 08542; *ahajian@princeton.edu.*
[2] Department of Astrophysical Sciences, Peyton Hall, Princeton University, Princeton, NJ 08544; *dns@astro.Princeton.edu.*
[3] Department of Physics and Astronomy, University of Pennsylvania, 209s 33rd str, Philadelphia, PA 19104; *carloshm@astro.upenn.edu; raulj@physics.upenn.edu;lverde@physics.upenn.edu.*

[4] Note that this will not be the case in a coordinate system where the CMB has a large dipole, like for example in a coordinate system where the Sun is at rest

low-DM pulsars, angular broadening of Galactic and extragalactic sources and emission measures to infer the distribution of the free electrons in the Galaxy responsible for pulsar dispersion measures and a spatial model of the warm ionized component of the interstellar gas.

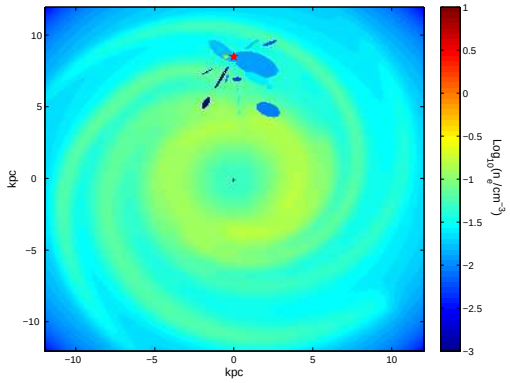

FIG. 1.— Distribution of the free electrons in our Galaxy, $log_{10}(n_e)$, based on NE2001. The n_e is shown at the Galactic plane, $z = 0$, and is maximum at the Galactic center. The position of the Sun is denoted by a star, $\star$, and the small overdense region close to the Sun is the Gum Nebula.

The electron density distribution is given by the sum of two axisymmetric components (the thick disk and the thin disk) and a spiral arm component, combined with terms that describe specific regions in the Galaxy. The local interstellar medium is modeled with multiple components: (a) four low density regions near the Sun: a local hot bubble centered on the Sun's location, the North Polar Spur, a local superbubble and another low density region, (b) the Galactic center component, (c) the Gum Nebula and the Vela Supernova Remnant, (d) regions of intense scattering (clumps) and (e) regions of low density (voids).

Figure 1 shows the Galactic distribution of the free electrons, n_e,at the Galactic plane, based on the NE2001 model. The position of the Sun is denoted by a red star. The high electron density spot on the left side of the Sun is the Gum nebula.

3. KINEMATICS OF THE DIFFERENTIAL ROTATION OF THE GALAXY

We consider an axisymmetric model for the rotation of the Milky Way. The orbits in this model are circular and the angular velocity at point $\mathbf{R}$ is $\mathbf{\Omega}(R)$, where $R = |\mathbf{R}|$. We are interested in the line-of-sight velocity, v_{los}, the projection of the velocity of each particle relative to the Sun along the vector connecting the Sun to that point, $(\mathbf{R} - \mathbf{R}_\odot)$. Here, $\mathbf{R}_\odot$ denotes the position of the Sun in the Galactocenteric coordinates. Therefore,

$$v_{los} = \hat{\mathbf{R}}_{los} \cdot (\mathbf{v}_{rot} - \mathbf{v}_\odot), \tag{4}$$

where $\hat{\mathbf{R}}_{los} = (\mathbf{R} - \mathbf{R}_\odot)/|\mathbf{R} - \mathbf{R}_\odot|$. Following the standard discussion in Binney & Merrifield (1998), the line of sight velocity v_{los} can be expressed as a function of longitude, l, on the celestial sphere and R

$$v_{los}(l, R) = [\Omega(R) - \Omega(R_\odot)]\, R_\odot \sin l. \tag{5}$$

The disk of the Milky Way consists of three parts: the central disk at $R < 3$ kpc, the inner disk, $R_0 > R > 3$ kpc and the outer disk, $R > R_0$. The determination of the v_{los} is different in each of the three parts.

For the inner disk, the observable is the terminal velocity, $v^t_{los}(l_1)$, along each line of sight, l_1. The terminal velocity is defined as follows: consider the smallest ring -centered on the galactic center- that intercepts the line of sight. The line of sight is thus tangent to this ring, and the radius of the ring is $R = R_\odot \sin l_1$. The terminal velocity is the line of sight velocity of the ring at the tangent point. 21-cm line and CO emission line observations are used to estimate v_{los} (e.g., Rougoor & Oort (1960)) and the distance to the tangent point is determined by geometry. The circular velocity of the ring can be calculated using $v^t_{los}(l)$ values reported in Chapter 9 of Binney & Merrifield (1998) and eq.(5),

$$v_c(R) = v^t_{los}(l_1) + v_c(R_0) \sin l_1, \quad \sin l_1 = R/R_0, \tag{6}$$

and therefore

$$v_{los}(l, R) = [v_c(R) \cdot R_0/R - v_c(R_0)] \sin l. \tag{7}$$

In the outer disk, distances are not so easily determined and thus distances and velocities are obtained either by observations of Cepheid variables or by main sequence fitting of a young cluster and radio-line observations of associated molecular gas (see Brand & Blitz (1993) and references therein).

The measurement of v_{los} is then given by

$$v_{los}(l, R) = W(R) \sin l, \tag{8}$$

where $W(R) \equiv R_0[\Omega(R) - \Omega(R_0)]$ is given as a function of R/R_0 in Brand & Blitz (1993). Note however that the errors associated to the distance R and the errors assigned to a given measurement of $W(R)$ increase dramatically for $R > 1.5R_0$, and therefore very little can be said about v_{los} for radii larger than $2R_0$, (Binney & Dehnen 1997).

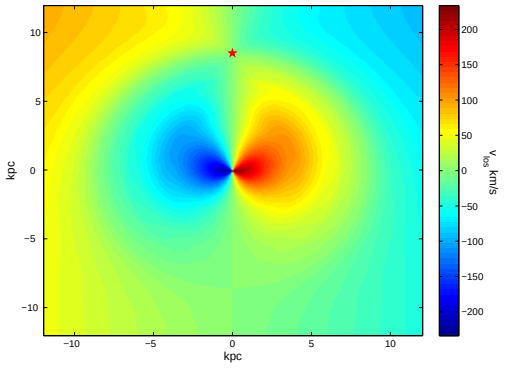

FIG. 2.— The line-of-sight velocity relative to the Sun, v_{los}, on the plane of the Galaxy.The position of the Sun is denoted by $\star$. v_{los} is negative when a point moves towards the Sun.

The velocities in the central disk are more complicated. Here, we calculate them in the same way as the inner disk velocities: we extrapolate the terminal velocities of the central disk from those of the inner disk. This approximation however does not significantly affect our final result because the v_{los} is small in the vicinity of the Galactic center. In addition, the effect of non-circular motions such as axisymmetric expansion, oval distortions

of the orbits and random motions, act as a correction to the above model. For simplicity we ignore these corrections and only consider circular motions: as discussed in Chapter 9 of Binney & Merrifield (1998), this simplified model works well outside of the central ($3kpc$) disk.

4. THE KINETIC SZ PATTERN

We now separately compute the contribution to the kSZ signal due to the rotation of the Galaxy (4.1) and the contribution due to the motion of the Galaxy with respect to the CMB rest frame (4.2). We use the free electron density model of NE2001 and the above model for the velocity field of the Galaxy to obtain the Galaxy kSZ pattern. As the velocity field, v_{los} is defined with respect to the Sun, there will be an additional contribution due to $\mathbf{v}_{dipole}$.

4.1. *Motion within the Galaxy*

We assume the Sun is located at $(x, y, z) = (0.0, 8.5, 0.0)$ kpc in Galactocenteric coordinates, $R_0 = 8.5$ kpc, and $v_\odot = 220$ km/s. The kSZ effect is calculated using eq.(2). We integrate eq.(2) along the line of sight:

$$\Delta T(\hat{n}) = -\frac{\sigma_T}{c} T_0 \sum_{i=1}^{N} n_e(r_i\hat{n}) v_{los}(r_i\hat{n}) \Delta r \qquad (9)$$

$$\simeq -(4.1\mu K) \sum_{i=1}^{N} \left(\frac{n_e(r_i\hat{n})}{1cm^{-3}}\right) \left(\frac{v_{los}(r_i\hat{n})}{220\mathrm{km/s}}\right) \left(\frac{\Delta r}{kpc}\right),$$

where $r_i = r_{i-1} + \Delta r$ with $r_0 = 0$. While the velocities in the outer disk are not known beyond $r \sim 1.5 - 2R_0$, most of the contribution comes from the central and inner disks, hosting the largest electron densities and peculiar velocities. Thus we only consider electrons that are within the $r = 2R_0$ sphere. The result is shown in Fig. 3. The kSZ pattern is antisymmetric: its main features are

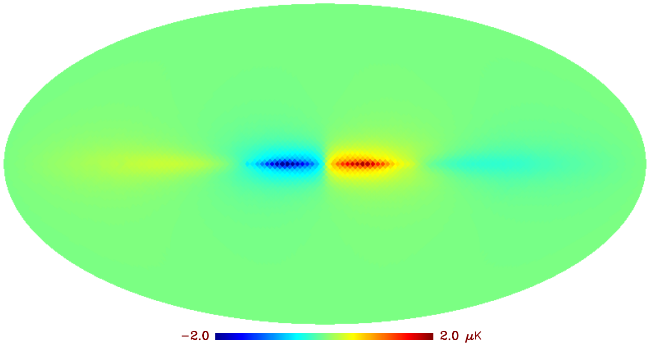

FIG. 3.— Map of the predicted kinetic SZ signal caused by the rotation of the free electrons in the disk of our Galaxy.

a cold and a hot spot at the two sides of the Galactic center with $|l| < 90°$ and $\delta T_{max} \sim 2\mu K$. These spots come from the regions in the inner disk with the highest v_{los} (see Fig. 2). There are weaker warm and cold spots at larger longitudes, $|l| > 90°$, caused by the rotating electrons in the outer disk. The kSZ signal is zero at $l = 0°$ and $l = 180°$ where $v_{los} = 0$. Both the Galactic center and the Gum Nebula, which have the larger n_e, happen to fall in regions with very small v_{los} and therefore do not contribute much to the kSZ due to the rotation of the Galaxy.

4.2. *Motion of the Galaxy*

The second term of eq.(3) arises from the bulk motion of the Galaxy with respect to the CMB rest frame. We consider the dipole velocity to be $v_{dipole} = 371km/s$ in the direction of $(l, b) = (264°, 48°)$. This bulk motion

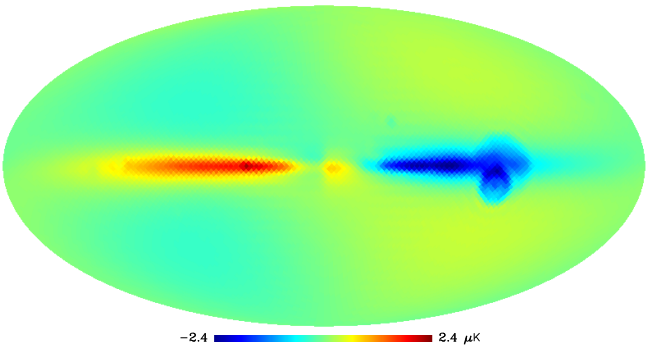

FIG. 4.— Dipole subtracted map of the effect of the free electrons in our Galaxy due to the rotation and the bulk motion of the Milky Way.

generates a kSZ signal bigger than the one due to the rotation of the Galaxy. The signal can be interpreted as a suppression of the dipole due to the free electrons in the Galaxy, thus it is a negative dipole modulated by the line of sight integration of the electron distribution n_e. The signal of the Galactic Center and the Gum nebula feature prominently because of their high density.

4.3. *The Combined effect*

We add this to the map of Figure 3 to obtain the total kSZ signal generated by the free electron distribution in our Galaxy. The resulting map *after dipole subtraction* is shown in Figure 4. This pattern is still antisymmetric and mostly lies in the plane of the Galaxy but it overrides the four-fold pattern of Figure 3. The cold spot centered at $(l, b) = (-90°, 0°)$ is due to the overdensity of the free electrons in the Gum Nebula and the warm spot at the center of the Galaxy reflects the high n_e there. Figure 5 shows the angular power spectrum of the kSZ signal. Most of the power resides at large scales (low l's), but its contribution to the intrinsic CMB power spectrum remains around the 0.01% level. An interesting feature of the above pattern is the saw-tooth shape of its angular power spectrum. This is due to the large-scale antisymmetry of the kSZ pattern which suppresses the even multipoles with respect to the odd ones. The pattern quickly disappears at higher multipoles.

5. DISCUSSION AND CONCLUSION

We have computed the kinetic SZ contribution to the CMB anisotropies due to the coherent motion of the free electrons in the disk of our Galaxy. We used the model of Cordes & Lazio (2002) for the galactic distribution of free electron and kinematics of the differential rotation of

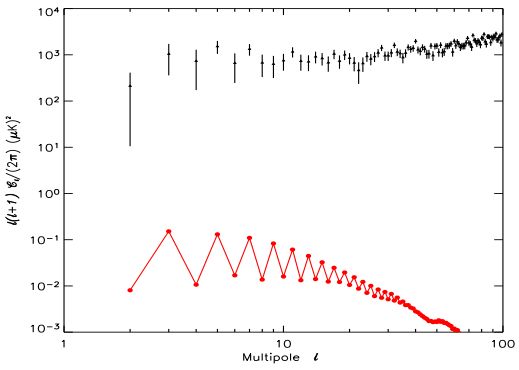

FIG. 5.— Angular power spectrum C_l for the predicted Kinetic SZ signal (red filled circles). Measurements from WMAP (3yr data) are displayed as black triangles.

our Galaxy to compute the line of sight velocity with respect to the Sun. The bulk motion of our Galaxy causes another effect that is comparable to this effect. We calculate the anisotropic pattern due to the combination of these effects and show the result in Fig. 4.

This kSZ signal is subdominant compared to the primary CMB and other foregrounds, but the model used to compute it has no free parameters and thus this contribution to the anisotropy can be easily modeled and subtracted out. This effect has been independently studied by another group (Waelkens et al. 2007) and our results agree. The polarization signal of the Thompson scattering from the free electrons in the local Universe was studied in Hirata et al. (2005). In Figure

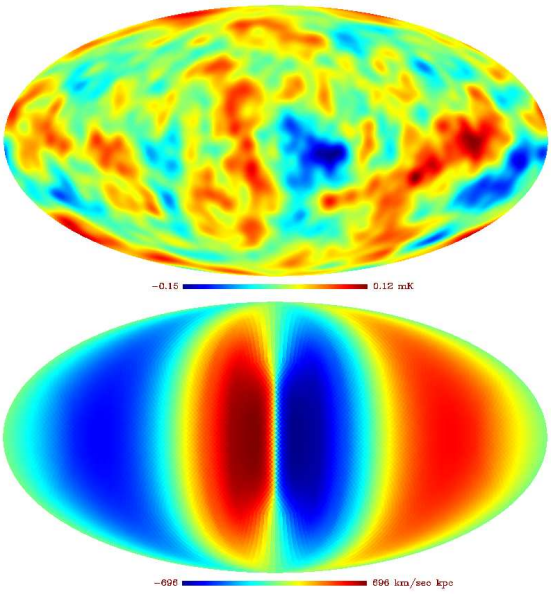

FIG. 6.— *top:* The ILC map based on the WMAP 3yr data, smoothed with a 420′ beam. *bottom:* A map of the integral of the line-of-sight velocity relative to the Sun in Galactic coordinates. Both maps happen to have a similar structure on the large scales.

6 we show WMAP's ILC map Hinshaw et al. (2006) smoothed with a 420′ beam and a map in galactic coordinates of the integral of the line of sight velocity due to the rotation of the Galaxy. Note the similarity between the maps. However, any scattering process would flip the sign of the radial velocities. We find another similarity in the saw-tooth pattern of the angular power spectrum of the kSZ map (Fig 5). This pattern has the same shape as the full-sky power spectrum derived from WMAP's ILC map: at low-l, even multipoles are suppressed with respect to the odd ones. Although the kSZ signal is too small to explain the suppression of the even multipoles in the WMAP data, it suggests that a mechanism that boosts the above kSZ signal by about two orders of magnitude might explain the saw-tooth pattern of the ILC power spectrum and other peculiarities of the two point correlation of the ILC map (such as the anticorrelation at $\theta = 180°$, Hajian et al. (2007); Hajian (2007)). Any element in our Galaxy that does not emit but only scatters CMB photons would be a good candidate for the above process, since it would preserve the thermal CMB spectrum and enhance the kSZ signal. We do not know any physical mechanism with the above properties.The intriguing similarity in figure 6 is, therefore more likely a warning about the dangers of *a posteriori* analysis than the signature of novel physics.

AH thanks Joseph Taylor and Andre Waelkens for enlightening discussions. Some of the results in this paper have been derived using the HEALPix package (Gorski et al. 2005). We acknowledge the use of the Legacy Archive for Microwave Background Data Analysis (LAMBDA). Support for LAMBDA is provided by the NASA Office of Space Science. AH acknowledges support from NASA grant LTSA03-0000-0090. LV and CHM are supported in part by NASA grant ADP03-0000-009 and ADP04-0000-093. RJ, LV, CHM and DNS are supported in part by NSF PIRE-0507768 grant. LV, RJ and CHM thank the Physics department of Princeton University for hospitality while part of this work was being carried out.

REFERENCES

Sunyaev, R. A., & Zeldovich, I. B. 1980, MNRAS, 190, 413
Hogan, C. J. 1992, ApJ, 398, L77
Binney, J., & Dehnen, W. 1997, MNRAS, 287, L5
Binney, J., & Merrifield, M. 1998, Galactic Astronomy, Princeton University Press, 1998.
Brand, J., & Blitz, L. 1993, A&A, 275, 67
Cordes, J. M., Lazio T., J., W., arXiv:astro-ph/0207156.
Gorski, K. M., Hivon, E., Banday, A. J., Wandelt, B. D., Hansen, F. K., Reinecke, M., Bartelman, M., Astrophys. J. **622**, 759 (2005)
Hajian, A., arXiv:astro-ph/0702723.
Hajian et al., in preparation.
C. M. Hirata, A. Loeb and N. Afshordi, Phys. Rev. D **71**, 063531 (2005) [arXiv:astro-ph/0501167].
Rougoor, G.W. & Oort, J.H., 1960, *Proc. Nat. Acad.Sci. 46, 1.*
Taylor J., H. , Cordes, J. M. , Astrophys. J. **411**, 674 (1993).
G. Hinshaw *et al.* [WMAP Collaboration], arXiv:astro-ph/0603451.
Waelkens et al. (2007) in preparation, (private communication).